# PATENT SPECIFICATION (11) 1387 173

1387 173

(21) Application No. 13290/72 (22) Filed 22 March 1972

(31) Convention Application No. 16292/71 (32) Filed 22 March 1971 in

(33) Japan (JA)

(44) Complete Specification published 12 March 1975

(51) INT CL² H01J 39/38

(52) Index at acceptance

H1D 21B 21D 21X

(19)

## (54) ENERGY ANALYZER OF THE COAXIAL CYLINDRICAL TYPE


(71) We, HITACHI LIMITED, of 1—5—1 Marunouchi, Chiyoda-ku, Tokyo, Japan, a body corporate organized according to the laws of Japan, do hereby declare

the invention, for which we pray that a patent may be granted to us, and the method by which it is to be performed, to be particularly described in and by the following statement: —

The present invention relates to energy analyzers of the coaxial cylindrical type, in which ultraviolet rays, X-rays, gamma rays, or similar rays are applied to a sample, and the energy of the charged particles, such as electrons and ions, emitted from the surface of the sample is analyzed.

In a conventional energy analyzer consisting of an outer cylindrical electrode and an inner cylindrical electrode disposed coaxial to each other, a voltage is applied across said outer and inner electrodes, and the charged particles from the sample member are analyzed in the energy dispersion field located between said outer and inner electrodes.

The charged particles, such as electrons and ions, are admitted into said energy dispersion field (or energy analyzing field) through an incidence slit disposed on the axis of said electrodes and focussed into a beam with an acceptance angle of $2\alpha$ through an angle-defining cylindrical slit disposed inside said inner cylindrical electrode. Then the beam enters said energy analyzing field through an axial gap in the wall of said inner electrode. The charged particles in the energy dispersion field are dispersed according to the magnitude of energy of the individual particles. The path of the charged particles in said dispersion field is a parabolic curve. The charged particles passing through said dispersion field enter a detecting slit, through another axial gap in the wall of said inner electrode, and thence reach the detector.

Among the charged particles passed through the dispersion field and subjected to energy dispersion, only those having a certain specific energy and therefore a certain incidence angle $\theta_o$ should be selected by the detecting slit and admitted into the detector. Hence the energy spectrum can be obtained when the strength of the energy dispersion field, i.e. the voltage applied across the inner and outer electrodes, is varied; or the energy of the charged particles, i.e. the voltage for accelerating the charged particles before entering the incidence slit, is varied; and the number of the charged particles reaching the detector is measured.

In a conventional energy analyzer, however, the charged particles from the incidence slit are focussed into a beam with an acceptance angle of $2\alpha$ and driven into the dispersion field, and as a result not only the charged particles having a specific energy but also those with an energy in the range corresponding to the incidence angle $\theta_o \pm \alpha$ reach the detector, to cause an aberration.

Such aberration, attributable to the acceptance angle $2\alpha$ of the incident beam, can be reduced by narrowing the angle-defining slit and thus decreasing the angle $\alpha$. If this method is used, however, the number of the charged particles reaching the detector is reduced, which results in a decrease in the intensity of the beam.

It is an object of the present invention to provide a coaxial cylindrical type energy analyzer operable at a high intensity.

According to the present invention there is provided an energy analyzer for analyzing the energy of charged particles including an outer cylindrical electrode, an inner cylindrical electrode coaxial with the outer electrode and having a first aperture for admitting the particles to the space between the electrodes from inside the inner electrode and a second aperture for re-admitting the particles to the inside of the inner electrode from the space, means for applying a voltage between the inner and outer electrodes, whereby the particles follow a curved path through the analyzer away from and then back towards the coaxis of the electrodes, a member having a cylindrical wall, said wall being

coaxial with the electrodes and being provided with an incidence slit from which slit the particles emerge towards the first aperture, an angle-defining slit adjacent the first aperture adapted to adjust the trajectories of the charged particles admitted to said space and a detecting slit axially spaced from the incidence slit through which slit the particles pass from the second aperture in order to reach a detector.

The present invention will now be described in greater detail by way of example with reference to the accompanying drawings, in which:—

Figure 1 is a schematic diagram illustrating the principles of a conventional coaxial cylindrical energy analyzer;

Figure 2 is a schematic diagram illustrating the principles of the present invention;

Figure 3 is a diagram showing the acceptance angle $2\gamma$ of the beam measured in the plane perpendicular to the coaxis of the electrodes in the analyzer shown in Figure 2;

Figure 4 is a graphic representation showing the relation between the incidence angle $\theta_o$ necessary for the second order focussing and the intensity $K_o$ of the dispersion field, using a parameter $\eta$ determined by the diameter of the detecting slit of Figure 2;

Figure 5 is a diagram showing by a curve the intensity distribution over the diameter of the detecting slit, of the charged particles reaching the detecting slit of Figure 2;

Figure 6 is a diagram showing by a curve the relation between the number of the charged particles passed through the detecting slit of Figure 2 and the deviation of the particle energy from the normal value thereof;

Figure 7 is a contour diagram showing the intensity of the beam of an analyzer constructed on the principles illustrated in Figure 2, optimized under secondary focussing condition; and

Figures 8(a) and 8(b) are sectional diagrams showing two preferred forms of energy analyzer.

Referring to Figure 1, a cylindrical inner electrode 1 and a cylindrical outer electrode 2 are disposed coaxial to each other, and a voltage $V_p$ is applied across the two electrodes 1 and 2, thereby forming a charged particle energy dispersion field 3 in the annular space between the inner and outer electrodes 1 and 2. An incident slit 5 of a circular shape with a diameter of $2\varepsilon\alpha$ is disposed on the axis of the electrodes. Charged particles such as electrons and ions are emitted from a sample member (not shown) irradiated with ultraviolet rays, X-rays or similar rays. The charged particles are driven into the analyzer through the slit 5 and formed into a beam with an acceptance angle of $2\alpha$ after being passed through a cylindrical angle-defining slit 6 disposed annularly inside the inner electrode 1. The beam is driven into the energy dispersion field 3 between the inner and outer electrodes 1 and 2 by way of a first axial gap in the wall of the inner electrode 1. In the dispersion field 3 the charged particles are dispersed according to the magnitudes of their energy. After curving back towards the inner electrode 1, the charged particles re-enter thereinto through a second axial gap in the wall thereof, and then reach a detector 8 via a detecting slit 7 disposed on the axis of the electrodes 1 and 2.

Among the charged particles passed through the energy dispersion field 3 and subjected to energy dispersion, those with a specific energy are selected by the detecting slit 7 and delivered to the detector 8. Hence, by varying the field strength of the dispersion field 3, i.e. the voltage $V_p$ applied across the inner and outer electrodes 1 and 2, or by varying the voltage for accelerating the charged particles before entering the incidence slit 5 and thereby varying the charged particle energy eVe, and at the same time measuring the number of the charged particles reaching the detector 8, the energy spectrum can be obtained.

In this case, the charged particles are driven into the dispersion field through the incidence slit 5 in the form of a beam with an acceptance angle of $2\alpha$ and, therefore, the actual trajectory of the charged particles deviates from a mean trajectory 9 of the charged particles with a specific energy and driven at the incidence angle $\theta_o$, by an angle $\alpha$ from the incidence angle $\theta_o$. The charged particles are driven into the dispersion field at an incidence angle $\theta \pm \alpha$, and not only the charged particles having a specific energy but also those with an energy in the range corresponding to the incidence angle $\theta \pm \alpha$ reach the detector 8, to cause an aberration.

Such aberration attributed to the acceptance angle $2\alpha$ of the incident beam can be reduced by narrowing the angle-defining slit 6 and decreasing the angle $\alpha$. On the other hand, however, the number of the charged particles reaching the detector 8 is reduced to result in decrease in the intensity.

It is to be assumed that the trajectory 9 is that followed by charged particles having a kinetic energy $E_o$ ($E_o = eVe$) and entering from an incidence point 10 on the axis of the incidence slit 5 into the energy dispersion field 3 at an incidence angle $\theta_o$ measured in an axial plane of the electrode, and another trajectory is followed by other charged particles having a kinetic energy E and driven into the energy dispersion field through the angle-defining slit 6. Then the deviation $f$ between the two trajectories in the axial direction at the detecting slit 7 is given in terms of expansion into power series as follows.

$$f=a(Dt+S+C\alpha_1\alpha+C\alpha_2\alpha^2+C\alpha_3\alpha^3+\ldots) \quad (1)$$

where Ci is the aberration coefficient

$$(i=\alpha_1,\ \alpha_2,\ldots,\gamma_2,\ldots,\alpha\gamma_2,\ldots)$$

D is the energy dispersivity

$$E=E_o\ (1+t)$$

incident angle $\theta=\theta_o+\alpha$

S will be defined below.

The aberration coefficient Ci and the value of energy dispersivity D are determined from equation (1) when the incident angle is $\theta_o$ and the strength of the energy dispersion field is $K_o \equiv Ve/Vp\ (\log b/a)$ (where $a$ is the radius of the inner cylindrical electrode 1, and $b$ is the radius of the outer cylindrical electrode 2). When $\theta_o=42.307°$ and $K_o=1.0310$, the first and second order aberration coefficients with respect to $\alpha$ are both zero.

In the prior art the incident slit 5 and the detecting slit 7 are disposed centering the axis of the cylindrical electrodes 1 and 2, and such incidence angle $\theta_o$ and analyzing field strength $K_o$ as will satisfy as far as the second order focussing condition with respect to $\alpha$ are used. In this type of analyzer, because the charged particles are driven thereinto through the incident slit 5 on the axis and focussed at the detection slit 7 on the same axis, substantially sufficient intensity can hardly be realized.

In Figure 2, a cylindrical incidence slit 25 is formed by an axial gap in the wall of a cylindrical member 23, which has a diameter of $2a\rho_1$, and a cylindrical detecting slit 27 is formed by an axial gap in the wall of a cylindrical member 24, which has a diameter of $2a\rho_2$. The cylindrical members 23 and 24 are coaxial with an inner cylindrical electrode 21 and an outer cylindrical electrode 22, across which electrodes a voltage Vp is applied, thereby forming the energy dispersion field 3 in the annular space between said two electrodes.

The incidence slit 25 and detecting slit 27 are distant from the axis 4 of the electrodes 21 and 22 and the members 23 and 24 by $a\rho_1$ and $a\rho_2$ respectively. The deviation $f$ in the axial direction on the detecting slit 27, between the trajectory 9 of the charged particles with a specific energy $E_o$, which particles are emitted from a point 10 on the incidence slit 25, and a trajectory of another charged particle is expressed as

$$f=a(Dt+S+C\alpha_1\alpha+C\alpha_2\alpha^2+C\alpha_3\alpha^3+C\gamma_2\gamma^2+C\alpha\gamma_2\alpha\gamma^2+\ldots) \quad (2)$$

where $\gamma$ represents half the acceptance angle of the beam measured in the plane perpendicular to the axis 4 and including the incidence point 10 on the incidence slit 25 of the standard trajectory 9, as shown in Figure 3, and S denotes the axial distance between the incidence point 10 of the standard trajectory on the incidence slit 25 and the incidence point of the other trajectory.

In this case also, the aberration coefficient Ci and the value of energy dispersivity D as in Eq. (2) are determined according to the beam incidence angle $\theta_o$ and the dispersion field strength $K_o$.

When $C\alpha_1=0$ in equation (2), the relation between the incidence angle $\theta_o$ and the field strength $K_o$ which are to satisfy the first order focussing condition for $\alpha$ is determined. When the incident angle $\theta_o$ and the field strength $K_o$ are varied under the first order focussing condition, it is possible to make the second order aberration coefficient $C\alpha_2$ zero ($C\alpha_2=0$) at specific values of $\theta_o$ and $K_o$ even if the positions $\rho_1$ and $\rho_2$ of the incident slit and the detecting slit are arbitrarily determined, or these positions are located at arbitrary distances from the axis. When the values of $\theta_o$ and $K_o$ to satisfy the second order focussing condition are assumed to be $\theta_o°$ and $K_o°$, the relation between $\theta_o°$ and $K_o°$ against a parameter $\eta$ will be as shown in Figure 4, where

$$\eta=1-\frac{1}{2}(\rho_1+\rho_2).$$

When the second order focussing condition is satisfied, the deviation $f$ between the standard trajectory and the other trajectory is expressed by equation (3) based on equation (2), assuming that higher order terms are negligible (practically the deviation $f$ is not appreciably affected by the higher order terms).

$$f=a(Dt+S+C\alpha_3\alpha^3+C\gamma_2\gamma^2+C\alpha\gamma^2\alpha\gamma^2) \quad (3)$$

When the width of the incident slit 25 is $2\alpha S_o$, the charged particle acceptance angles measured respectively parallel and perpendicular to the axis + are $2\alpha_o$ and $2\gamma_o$, and the energy is E ($E=E_o\ (1+t)$), the intensity distribution J $(u, t)$ of the charged particles reaching the plane of the detecting slit is determined as shown in Figure 5. When the width of the detecting slit 27 is $2d_o$, the number of the charged particles passing through the detecting slit 27 is given as the

function I(t) of the energy E, by Equation (4) below.

$$I(t)=\int_{-do}^{do} J(u, t)\, du \qquad (4)$$

This relation is illustrated in Figure 6. In equation (4), $u$ and $do$ represent the values normalized from the actual length based on the radius $a$ of the inner electrode.

The resolving power of the analyzer is expressed by the base width of the spectral line $I(t)$, i.e., the width $t_2-t_1$, and the intensity is given by the integral area of the spectral line $I(t)$. The resolving power $\Delta$ and the intensity L are expressed as

$$\Delta=do+f\ \max+f\ \min \qquad (5)$$

$$L=\frac{2^4 So\ do\ \alpha o\ \gamma o \sin\theta_o}{D}\cdot a^2 \qquad (6)$$

where $f$ max and $f$ min are the maximum and minimum values, respectively, of Eq. (3) when S, $\alpha$, $\gamma$ are varied in the variable range of $\pm So$, $\pm\alpha o$ and $\pm\gamma o$ which are determined by the individual slits.

The optimum values of So, $do$, $\alpha o$ and $\gamma o$ which determine the slit width and beam acceptance angle are selected so that the resolving power $\Delta$ is kept constant and the intensity L is maximized. These optimum values are calculated as follows by Lagrange's method of undetermined multipliers. When

$$\psi=\Delta-\mu L$$

(where $\mu$: undetermined multiplier),

$$\frac{\delta\psi}{\delta So}=\frac{\delta\psi}{\delta do}=\frac{\delta\psi}{\delta\alpha o}=\frac{\delta\psi}{\delta\gamma o}=0 \qquad (7)$$

From Eq. (7), each of the optimum values of $S_o$, $d_o$, $\alpha_o$ and $\gamma_o$ is given by the following equations.

$$C\alpha_3\alpha^3{}_o=-\frac{D}{17}\cdot\frac{1\mp\frac{1}{2}\lambda\alpha_o}{1\mp\frac{16}{17}\lambda\alpha_o} \qquad (8)$$

$$\lambda\equiv\frac{C\alpha\gamma^2}{C\gamma_2} \qquad (9)$$

$$S_o=\frac{3}{17}D\Delta\cdot\frac{1\mp\lambda\alpha_o}{1\mp\frac{16}{17}\lambda\alpha_o} \qquad (10)$$

$$d_o=S_o \qquad (11)$$

$$C\gamma_2\gamma^2=\pm\frac{3}{17}D\Delta\cdot\frac{1}{1\mp\frac{16}{17}\lambda\alpha_o} \qquad (12)$$

Note that the above calculations are based on the condition that $\eta\leqq 1.0$.

The optimum condition for maximizing the intensity L under the condition that the resolving power $\Delta$ is constant is given by equation (8) to (12). The double sign in each of these equations depends on the sign of $\rho_2$.

In other words, the intensity L under the optimum condition depends on whether the detecting slit is located above or below the axis with respect to the incident slit, or depends on the position of the detecting slit with respect to the incident slit. This principle is illustrated in Figure 7 wherein the abscissa stands for the position $\rho_1$ of the incident slit against the axis, and the ordinate for the position $\rho_2$ of the detecting slit. The curves show in contour the intensity L under the optimum condition when the resolving power of the analyzer is set at $1\times10^{-2}$. When the position $\rho_2$ of the detecting slit is negative, this means that the position of the detecting slit is opposite to the incidence slit with respect to the axis. Namely, the focussing point (i.e. the position where the detecting slit is located) of the charged particles emitted from the incidence slit is positioned opposite to the incidence slit across the axis.

As will be apparent from Figure 7, in the coaxial cylindrical type energy analyzer used under the second order focussing condition, greater intensity L can be obtained by locating the detecting slit (i.e. the charged particle focussing point) opposite to the incident slit with respect to the axis.

Thus, according to the invention, a highly practical energy analyzer free of the prior art problems is realized.

Referring to Figure 8(a), there is schematically shown the structure of an energy analyzer embodying this invention wherein an outer cylindrical electrode 81 and an inner cylindrical electrode 82 with radius $a$ and $b$ respectively are disposed coaxial to each other, forming therebetween a space to serve as an energy dispersion field 83. Apertures 812 and 813 are disposed on the inner cylin-

drical electrode, through which apertures the charged particles to be analyzed pass.

A voltage $V_p$ whose magnitude can be varied is applied between the outer electrode 81 and the inner electrode 82. A cylindrical incidence slit is formed by an axial gap in the wall of a first cylindrical member 85 with a diameter $2a\rho_1$ installed coaxial to said cylindrical electrodes 81 and 82. A cylindrical detecting slit is formed by an axial gap in the wall of a second cylindrical member 87 with a diameter $2a\rho_2$ installed coaxial to said cylindrical electrodes 81 and 82. An angle-defining slit 86 is disposed in the neighbourhood of the aperture 812 inside the inner cylindrical electrode 82.

A focussing electrode 811 for introducing the charged particles from the detecting slit 87 into a detector 88 is disposed inside the inner cylindrical electrode 82. The numeral 814 denotes a sample member which is irradiated by ultraviolet rays, X-rays, gamma rays, corpuscular beam or similar rays whereby charged particles are produced. The detector 88 comprises in combination a scintillator and a photoelectronic multiplier to be operable at a high sensitivity.

This energy analyzer is operated in the following manner. The stream of charged particles emitted from the sample number 814 by way of the incidence slit is led into the space between the cylindrical electrodes through the aperture 812 at an incidence angle $\theta_o$ determined by the angle-defining slit 86. In the energy dispersion field 83 the charged particles are dispersed according to the magnitudes of energy the individual charged particles possess. Then the charged particles pass through the aperture 813, drawing a parabolic curve on either side of the mean trajectory. The charged particles after the aperture 813 cross the axis 84 of the electrodes 81 and 82 and the members 85 and 87 and are converged at the detecting slit on the side thereof located diametrically opposite to the side of the incidence slit from which the particles emerged.

The charged particles detected by the detecting slit are focussed by the focussing electrode 811 and thence introduced into the detector 88.

When the voltage $V_p$ applied between the inner and outer cylindrical electrodes 81 and 82 is varied, only the charged particles having a specific energy cross the axis and reach the detector, which then detects such charged particles. By the output of the detector, therefore, it becomes possible to measure the number of the charged particles and to obtain the energy spectrum.

The incidence slit 85 is located distant from the axis 84 and the detecting slit also is distant from the axis 84 and detects across the axis 84 the charged particles emitted from the incidence slit 85. In this structure the positions of the incidence slit and detecting slit can be expressed by $\rho_1$ and $\rho_2$ respectively, and the values $\eta$ of $\rho_1$ and $\rho_2$ can be suitably determined in the following ranges.

$$0<\rho_1<1$$

$$-1<\rho_2<0$$

When, for example, $\rho_1=0.55$ and $\rho_2=0.55$, the value of $\eta$ is 1. Hence, as shown in Figure 4, the value of the incident angle $\theta_o$ and the value of the dispersion field strength $K_o$ are:

$$\theta_o=42.3°$$

$$K_o=1.31$$

Under this condition the aberration coefficients $C\alpha_3$, $C\gamma_2$ and $C\alpha\gamma_2$, and energy dispersivity D are as follows.

$$C\alpha_3=-15.5$$

$$C\gamma_2=-0.4$$

$$C\alpha\gamma_2=2.0$$

$$D=5.6$$

Table 1 shows the optimum values obtained by using these values. In the foregoing embodiment the incidence slit width $2S_o$ and the detecting slit width $2d_o$ are based on the length along the axis of the analyzer (Figure 2). While in Table 1 these slit widths are indicated by $S_o'$ and $d_o'$ terms of length perpendicular to the standard trajectory.

TABLE 1

| $\Delta$ | $S_o'$, $d_o'$ | $\alpha_o$(rad) | $\gamma_o$(rad) | L |
|---|---|---|---|---|
| $1\times10^{-2}$ | $6.49\times10^{-3}$ | $6.32\times10^{-2}$ | $1.85\times10^{-1}$ | $4.85a^2\times10^{-6}$ |
| $1\times10^{-3}$ | $6.60\times10^{-4}$ | $2.83\times10^{-2}$ | $5.29\times10^{-2}$ | $6.42a^2\times10^{-2}$ |

In comparison with the data in Table 1, Table 2 shows those obtained in the conventional coaxial cylindrical type energy analyzer having the incidence slit and the detecting slit disposed on the axis 84. In this case, $\rho_1=\rho_2=0$ and, therefore $\eta=1.0$ as in the foregoing embodiment wherein the incidence slit and the detecting slit are not disposed on the axis 84. The values in Table 2 are obtained under the same focussing condition as in the foregoing embodiment of the invention.

TABLE 2

| Δ | ε | $\alpha_0$(rad) | L |
|---|---|---|---|
| $1\times10^{-2}$ | $9.56\times10^{-5}$ | $7.67\times10^{-2}$ | $6.47a^2\times10^{-7}$ |
| $1\times10^{-3}$ | $9.56\times10^{-4}$ | $3.56\times10^{-2}$ | $2.75a^2\times10^{-10}$ |

Based on the results of Tables 1 and 2, the intensity of the conventional analyzer in which the incidence slit and the detecting slit are disposed on the axis 84 is compared with that of the analyzer of this invention. The values shown in Tables 1 and 2 are obtained on condition that the resolving powers Δ are $1\times10^{-2}$, and $1\times10^{-3}$ respectively. When the resolving power Δ is $1\times10^{-2}$, the intensity is greater by 7.5 times in the analyzer of this invention than in the conventional analyzer. When the resolving power is $1\times10^{-3}$, the intensity is 23.3 times greater in the analyzer of this invention than in the conventional one.

In the foregoing embodiment, the incidence slit and the detecting slit are disposed outside the coaxis of the inner and outer cylindrical electrodes. The invention is not limited to this embodiment. For example, only the detecting slit may be disposed on the axis, and the charged particles emitted from the incidence slit may be detected at the point where the charged particles cross the axis. In this case, $\rho_2=0$, and the values of $\rho_1$ and $\rho_2$ are suitably determined in the following ranges.

$$0<\rho_1<1$$

$$-1<\rho_2\leqq O$$

Figure 8(b) shows part of another embodiment of the invention wherein the detecting slit 87 is disposed on the axis 84, and the charged particles are focussed at the point where the charged particles cross the axis 84. In Figure 8(b), the detecting slit portion is essentially illustrated in connection with the analyzer as in Figure 8(a), and the similar parts are not shown.

An analyzer constructed according to any of the above preferred forms is capable of energy analyzing in a very short time, since the intensity of the beam is not reduced during the passage of the beam through the analyzer.

WHAT WE CLAIM IS:—

1. An energy analyzer for analyzing the energy of charged particles including an outer cylindrical electrode, an inner cylindrical electrode coaxial with the outer electrode and having a first aperture for admitting the particles to the space between the electrodes from inside the inner electrode and a second aperture for re-admitting the particles to the inside of the inner electrode from the space, means for applying a voltage between the inner and outer electrodes, whereby the particles follow a curved path through the analyzer away from and then back towards the coaxis of the electrodes, a member having a cylindrical wall, said wall being coaxial with the electrodes and being provided with an incidence slit from which slit the particles emerge towards the first aperture, an angle-defining slit adjacent the first aperture adapted to adjust the trajectories of the charged particles admitted to said space and a detecting slit axially spaced from the incidence slit through which slit the particles pass from the second aperture in order to reach a detector.

2. An energy analyzer according to claim 1, wherein the detecting slit is cylindrical and coaxial with the electrodes, and the charged particles pass through the detecting slit before reaching the said coaxis, which axis the particles cross at a point of focus.

3. An energy analyzer according to claim 1, wherein the detecting slit is cylindrical and coaxial with the electrodes, and the charged particles cross the said coaxis before reaching the detecting slit, and after passing through the detecting slit the particles are curved back towards and focussed on the said coaxis by a focussing device.

4. An energy analyzer according to claim 1, wherein the detecting slit is an aperture on the said coaxis and the charged particles simultaneously pass through the detecting slit and cross the coaxis, and the particles are then curved back towards and focussed on the said coaxis by a focussing device.

5. An energy analyzer substantially as herein described with reference to and as illustrated in Figure 2 or Figure 8(a) or Figure 8(b) of the accompanying drawings.

MEWBURN ELLIS & CO.,
Chartered Patent Agents,
70—72 Chancery Lane,
London W.C.2.
Agents for the Applicants.

Printed for Her Majesty's Stationery Office, by the Courier Press, Leamington Spa, 1975.
Published by The Patent Office, 25 Southampton Buildings, London, WC2A 1AY, from which copies may be obtained.

FIG. 1

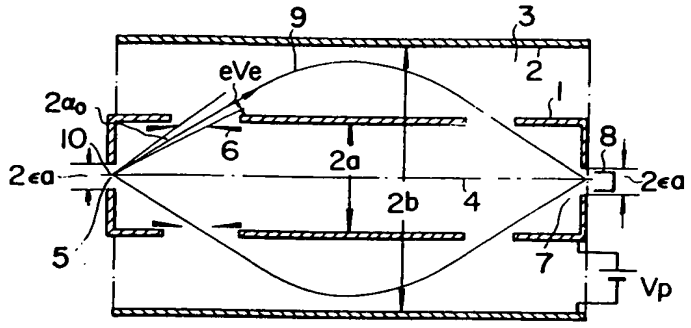


FIG. 2

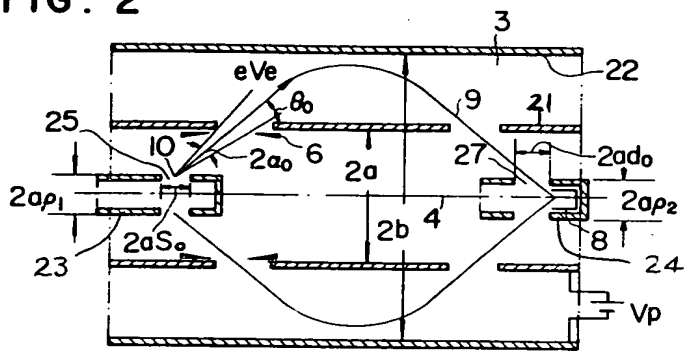


FIG. 3

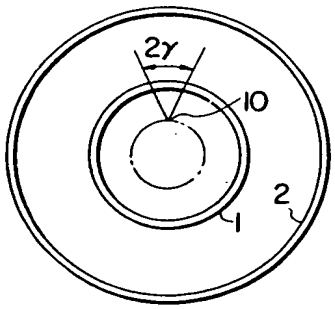

THIS PAGE BLANK (USPTO)

FIG. 4

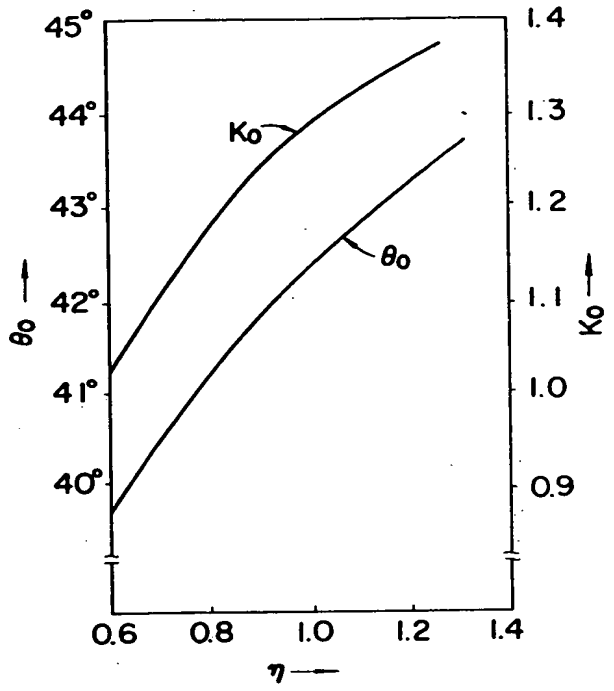
45°
44°
43°
42°
41°
40°
θo
1.4
1.3
1.2
1.1
1.0
0.9
Ko
Ko
θo
0.6
0.8
1.0
1.2
1.4
η

FIG. 5

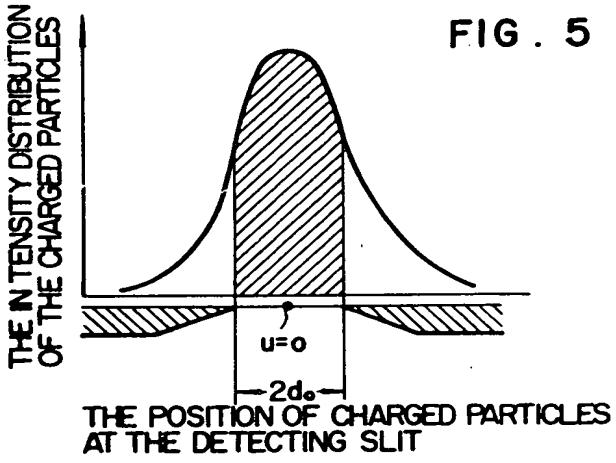
THE INTENSITY DISTRIBUTION OF THE CHARGED PARTICLES
u=o
2do
THE POSITION OF CHARGED PARTICLES AT THE DETECTING SLIT

THIS PAGE BLANK (USPTO)

FIG. 6

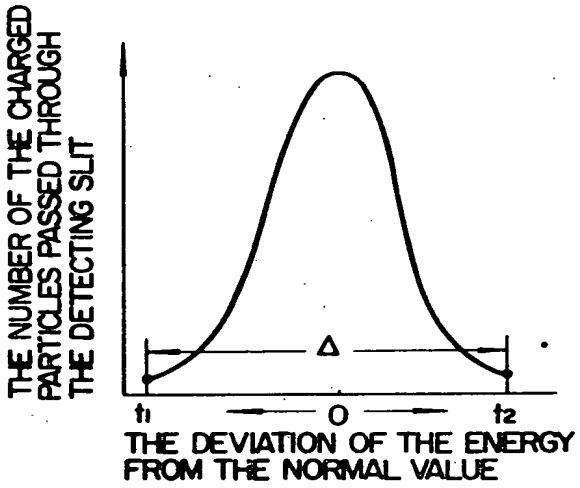
THE NUMBER OF THE CHARGED PARTICLES PASSED THROUGH THE DETECTING SLIT
Δ
t1
0
t2
THE DEVIATION OF THE ENERGY FROM THE NORMAL VALUE

FIG. 7

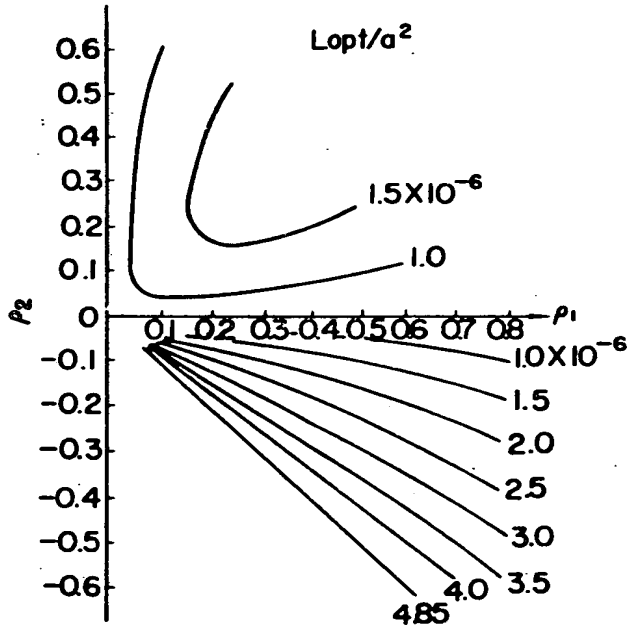
Lopt/a²
0.6
0.5
0.4
0.3
0.2
0.1
0
-0.1
-0.2
-0.3
-0.4
-0.5
-0.6
ρ2
ρ1
0.1 0.2 0.3 0.4 0.5 0.6 0.7 0.8
1.5X10⁻⁶
1.0
1.0X10⁻⁶
1.5
2.0
2.5
3.0
3.5
4.0
4.85

THIS PAGE BLANK (USPTO)

FIG. 8a

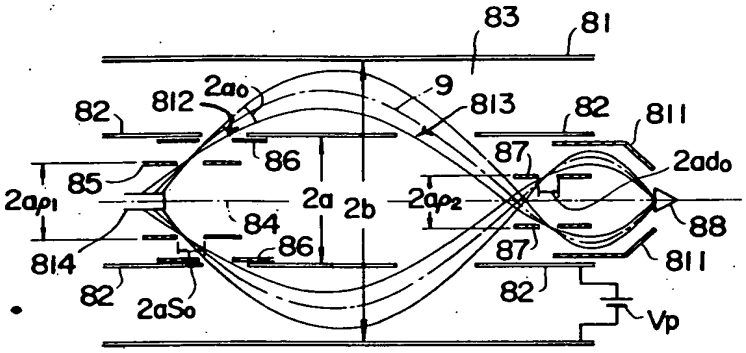
83
81
812
2a0
9
813
82
811
82
87
86
2ado
85
2aρ1
2a
2b
2aρ2
88
84
86
87
814
811
82
2aS0
82
Vp

FIG. 8b

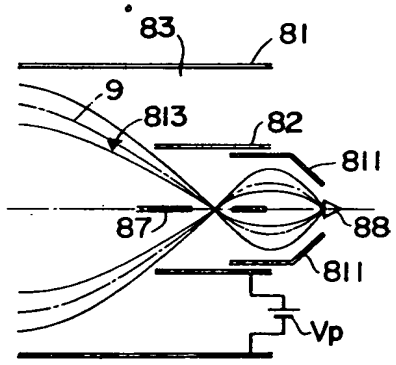
83
81
9
813
82
811
87
88
811
Vp

THIS PAGE BLANK (USPTO)